How long does it take to cue a *Pseudomonas aeruginosa* chronic infection phenotype in the lab? Insights from transcriptome analysis in a cystic fibrosis lung model.

Niamh E. Harrington[1,2*], Freya Allen[1,3], Ramón Garcia Maset[4,5], Freya Harrison[1*]

1: School of Life Sciences, Gibbet Hill Campus, The University of Warwick, Coventry, CV4 7AL, UK.

2: Department of Evolution, Ecology and Behaviour, Institute of Infection, Veterinary and Ecological Sciences, University of Liverpool, Liverpool, L69 7ZB, UK.

3: (Current address) Institute of Microbiology and Infection and Department of Microbes, Infection and Microbiomes, School of Infection, Inflammation and Immunology, College of Medicine and Health, University of Birmingham, Birmingham, B15 2TT, UK.

4: Warwick Medical School, Gibbet Hill Campus, The University of Warwick, Coventry, CV4 7AL, UK.

5: (Current address) Department of Engineering Science, University of Oxford, Parks Road, Oxford, OX1 3PJ, UK

* Co-corresponding authors: Niamh.Harrington@liverpool.ac.uk, F.Harrison@warwick.ac.uk

Keywords: Biofilm, chronic infection, cystic fibrosis, *ex vivo* model, *Pseudomonas*

aeruginosa, RNA sequencing, transcriptome, quorum sensing, antimicrobial resistance, sulfur metabolism

Abstract

The opportunistic pathogen *Pseudomonas aeruginosa* forms biofilm infections in the lungs of people with the genetic condition cystic fibrosis (CF) that can persist for decades. There are numerous *P. aeruginosa* lifestyle changes associated with chronic biofilm infection cued by the CF lung environment. These include a loss of virulence, metabolic changes and increased antimicrobial tolerance. We have investigated *P. aeruginosa* PA14 biofilm infection over 7 d in an *ex vivo* pig lung (EVPL) model for CF, previously shown to facilitate formation of a clinically relevant *P. aeruginosa* biofilm structure with expression of key genes comparable to human infection. We have compared *P. aeruginosa* gene expression between sequential time points: 24 h, 48 h and 7 d post infection, and investigated tolerance to polymyxins. Our results demonstrate that the EVPL model can maintain a *P. aeruginosa* biofilm population, which exhibits increased antibiotic tolerance, for at least 7 d. Differential expression of antimicrobial resistance-associated genes was not observed, however there was significant upregulation of sulfur metabolism and maintenance of a structured biofilm. Our findings provide further insight into the increased *P. aeruginosa* antibiotic tolerance during chronic infection of the CF lung, and suggest we can cue aspects of chronic infection in 7 d under the right lab conditions.

Introduction

Pseudomonas aeruginosa chronic biofilm infections of the cystic fibrosis (CF) lung are, in part, characterised by their physiological adaptations to the environment. This is driven by

environmental pressures such as osmotic, nitrosative and oxidative stress, as well as interactions with the commensal microbiome and co-infecting pathogens, and antibiotic exposure [1]. Lifestyle changes have been shown to improve *P. aeruginosa* persistence in the lung, including loss of swimming motility, impaired pyoverdine production, increased adherence and formation of a biofilm matrix that protects the bacterial cells from not only the host immune response, but also antibiotics [2, 3]. Quorum sensing (QS) largely controls the phenotypic changes observed in the biofilm population, and is estimated to influence expression of approximately 10% of all *P. aeruginosa* genes [4]. Initial physiological changes that induce a chronic, antibiotic-tolerant biofilm phenotype are followed by evolutionary changes in the population over years of infection. Late stage infections exhibit reduced phenotypic diversity and loss of virulence compared with early stage infections [5]. The reduction in virulence factor production is linked with a decline in expression of QS-related genes [6]. Once established, chronic *P. aeruginosa* infections are almost impossible to eradicate due to high levels of antibiotic resistance and tolerance, contributed to by the protective biofilm matrix.

Studies have shown that current *in vitro* models do not accurately represent critical aspects of *P. aeruginosa* chronic infection; in particular, QS-associated gene expression in CF sputum is not well captured [7]. However, our previous work has indicated that an *ex vivo* pig lung (EVPL) model may more accurately capture *in vivo* QS regulated gene expression over a short infection time (48 h) [8]. Our study focused on *P. aeruginosa* gene expression at 24 h and 48 h post infection (PI) in the EVPL model compared with *in vitro* synthetic cystic fibrosis sputum media (SCFM) growth. We found that the EVPL bronchiolar tissue-associated biofilm

formed at 48 h exhibited key characteristics of *in vivo* chronic infection not observed *in vitro* [8].

We now aim to build upon these findings to determine whether the EVPL model is viable for an extended infection time of 7 days, as a longer infection period may more accurately replicate chronic CF infections. We previously showed *P. aeruginosa* biofilms to have a clinically realistic, mature structure in the model at 7 days post infection [9]. We have now performed differential expression analysis and Kyoto Encyclopedia of Genes and Genomes (KEGG) pathway enrichment analysis. This confirms that the biofilm population was maintained at 7 d with limited stress and allows us to better understand expression changes in established biofilms and further knowledge of *P. aeruginosa* gene expression in later stage infections. We identified changes in several genes and pathways, including upregulation of sulfur metabolism and biofilm maintenance, that accompanied increased antibiotic tolerance over time. Our findings provide new insight into *P. aeruginosa* gene expression changes in an established biofilm infection and their potential implications for treatment success, as well as highlighting a viable extended time point for use of the EVPL model to study chronic *P. aeruginosa* biofilm infection in CF.

Methods

Bacterial strain. The *Pseudomonas aeruginosa* PA14 wild type strain used for this work was originally from the University of Washington [10, 11], and was grown on Lysogeny Broth (LB) agar (Melford Laboratories) for 24 h at 37 °C prior to all experiments.

Synthetic cystic fibrosis sputum medium. SCFM was made based on the original recipe by Palmer *et al.*, now commonly referred to as "SCFM1" [12]. Glucose was removed from the recipe as previous work using the EVPL model demonstrated that in the presence of lung tissue, the absence of glucose did not affect *P. aeruginosa* growth but did facilitate endogenous lung bacterial species growth [13].

EVPL dissection and infection. Pig lung bronchiolar tissue was dissected and subsequently infected following the previously published method [8, 9, 14]. Two independent lungs were used per experiment, with three individual tissue pieces used per lung. All lungs used for this work were provided by Steve Quigley and Sons Butchers Ltd. (Cubbington, United Kingdom) and were dissected and infected on the day of arrival from the abattoir.

EVPL antibiotic treatment. Two different antibiotics were tested: colistin and polymyxin B, both prepared as master stocks as follows: colistin (Acros Organics) was prepared to 10 mg ml^{-1} in dH_2O, and polymyxin B (Sigma-Aldrich) was prepared to 50 mg ml^{-1} in dH_2O. The master stocks of each antibiotic were further diluted in SCFM, in 15 ml Falcon tubes, to the desired concentration of 256 µg ml^{-1} for use with the EVPL model.

The EVPL grown biofilms were treated with each antibiotic as previously described [14]. Following incubation at 37 °C for either 24 h, 48 h, or 7 d, *P. aeruginosa* PA14 infected pig lung tissue pieces were removed from the individual wells of a 24-well plate using flame sterilised forceps. Each tissue piece was washed in 500 µl PBS in individual wells of a 48-well plate to remove non-biofilm associated bacterial cells. The tissue pieces were then transferred to individual wells of a 48-well plate, each containing 500 µl of either 256 µg ml^{-1}

colistin or 256 µg ml^{-1} polymyxin B. A replicate control, non-antibiotic treated set of tissue pieces from each lung per experiment, were transferred to individual wells of a 48-well plate each containing 500 µl PBS. All plates were covered with a UV sterilised Breathe-Easier® sealing membrane (Diversified Biotech), and incubated stationary at 37 °C for 24 h.

EVPL biofilm recovery and determination of bacterial load. Bacteria were recovered from the EVPL tissue pieces, and the bacterial load determined following the published method [8, 9, 14]. Briefly, following the final incubation for both RNA extractions and antibiotic treatments, tissue pieces were transiently washed in 500 µl PBS in individual wells of a 48-well plate to remove non-biofilm bacterial cells. Each tissue piece was then transferred into individual, sterile homogenisation tubes (Fisherbrand) containing 1 g of 2.38 mm metal beads (Fisher Scientific) and 1 ml PBS. The tissue-containing bead tubes were placed in a FastPrep-24 5G (MP Biomedicals), and bead beaten for 40 s at 4 m s^{-1} to recover bacterial cells from the lung-associated biofilm.

The lung homogenate was then used to determine the biofilm bacterial load associated with the EVPL tissue. An aliquot of each homogenate was serially dilute in PBS in a 96-well plate to final volumes of 200 µl. The dilutions were then plated in triplicate on LB agar and incubated overnight at 37 °C. The number of colonies of the two highest dilutions that were countable were determined and used to calculate the colony forming units (CFU) $lung^{-1}$ for each sample.

RNA extraction and sequencing, and relationship to previously published work. All RNA samples used for this work were collected as part of a bigger study, and thus the protocol

143 for extraction, precipitation, DNA removal and sequencing are outlined in the original
144 publication [8].
145
146 **RNA-sequencing bioinformatic analyses.** All reads were quality checked using FastQC
147 v0.11.8 [15] initially and following every processing step. Read trimming was performed
148 using Trimmomatic v0.38 [16] and a minimum read length threshold of 25 bp [7]. Residual
149 eukaryotic and bacterial rRNA were filtered out of the reads using SortMeRNA v2.1b [17],
150 then the remaining reads were mapped to the pig genome (*Sus scrofa*: NCBI,
151 GCF_000003025.6) using HISAT2 v2.1.0 [18]. All reads that aligned were removed using
152 Seqtk v1.3-r106 [19], and the remaining reads were aligned to the *P. aeruginosa* UCBPP-
153 PA14 genome (NCBI, GCF_000014625.1) using BWA v0.7.17-r1188 aligner with the MEM
154 algorithm [20]. The reads mapped to coding sequences were counted using the
155 "featureCounts", part of the Rsubread v2.0.1 R package [21], against the *P. aeruginosa*
156 UCBPP-PA14 annotation from pseudomonas.com [1]. Count data was normalised using the
157 rlog transformation function, part of the R package DESeq2 v1.26.0 [22]. Principal
158 component analysis (PCA) was then performed using the "plotPCA" function within DESeq2,
159 using genes (n = 5,829), and 95% confidence ellipses added using ggpubr v0.4.0 [23].
160
161 Differential expression analysis comparing the three time points: 24 h, 48 h, and 7 d, was
162 performed using the R package DESeq2 [22]. The threshold for significant differential
163 expression was an adjusted *P* value < 0.05 (Benjamini-Hochberg procedure to control the
164 false discovery rate) and log2 fold change ≥ |1.5|. A Venn diagram of the numbers of
165 differentially expressed genes was produced using VennDiagram v1.7.0 R package [24].
166 KEGG pathway enrichment analysis was then performed using the differentially expressed

genes using the “enrichKEGG” function from the clusterProfiler v3.14.3 R package [25] and the organism KEGG code “pau” for *P. aeruginosa* UCBPP-PA14. A KEGG pathway was considered significantly enriched if the adjusted *P* value < 0.05 (Benjamini-Hochberg procedure). The antimicrobial resistance genes studied were sourced from pseudomonas.com [1], using the Comprehensive Antibiotic Resistance Database (CARD) predictions [26]. Genes associated with the specific pathways: quorum sensing and biofilm formation, were sourced from the KEGG database [27-29].

Scanning electron microscopy. Following EVPL dissection, infection with *P. aeruginosa* PA14, and incubation at 37 °C for either 24 h, 48 h, or 7 d, lung tissue samples were fixed in 0.5 ml 2.5% glutaraldehyde solution in PBS, in a 24-well plate at 4 °C overnight. Uninfected tissue was also prepared as a negative control for *P. aeruginosa* infection.

Subsequently the 2.5% glutaraldehyde solution was removed, and the tissue samples were rinsed with PBS three times. Each tissue piece was then transferred to individual wells of a new 24-well plate and passed through an ethanol gradient at the following concentrations (v/v): 20%, 50%, 70%, 90%, 100%, and a further 100%, each for 1 h. The samples were transferred to individual wells of a further 24-well plate, and 0.5 ml hexamethyldisilazane (Electronic grade, 99+%) (HDMS) (VWR International Ltd) was added. The plate was incubated at room temperature for 3 h, then the HDMS solution was discarded. The tissue pieces were transferred to a new 24-well plate and left to dry in a laminar flow cabinet for 1 h. Double-sided copper tape (Agar scientific) was added to the scanning electron microscopy sample holders (Agar scientific), then the tissue samples were placed on top. All samples were then sputtered with carbon by using a carbon coater (SC7620 Mini Sputter

Coater/Glow Discharge System) and immediately imaged using a Zeiss Gemini scanning electron microscope with an InLens detector, at a voltage of 1 kV. The data was analysed using Omero5.6 [30].

Data presentation and statistical analyses. All bar graphs were produced using DataGraph v4.7.1 [31] on Mac OS Mojave v10.14.6. Analysis of variance (ANOVA) was performed on antibiotic treatment CFU data and post-hoc Tukey HSD tests. All statistical analyses including ANOVA and differential expression analysis were performed using RStudio v1.2.1335 (www.rstudio.com) on Mac OS Mojave v10.14.6.

Data availability. A full list of the significant DEGs from the three contrasts reported are provided as a data supplement. The raw sequence data is available at the European Nucleotide Archive (accession number: PRJEB48552).

Results

As reported in our previous study [8], we grew *P. aeruginosa* PA14 as a biofilm associated with the surface of EVPL bronchiolar tissue from two independent pig lungs for 24 h, 48 h and 7 d, and performed RNA sequencing from the recovered tissue-associated biofilm population. Our previous work confirmed that PA14 was still metabolically active 7 d PI, using an ATP-based viability assay (ref. [8] Figure S3), and the bacterial load was maintained; recovered CFU lung^{-1} 7 d PI were comparable to 24 h and 48 h PI (ref. [8] Figure S4). In the present study, we have extended our previous work to investigate *P. aeruginosa* PA14 gene

214 expression changes in the EVPL tissue-associated biofilm 24h – 7d PI ($P < 0.05$, $\log_2$ fold
215 change ($|\log_2 FC|$) ≥ 1.5). For all comparisons the earlier time point was used as the baseline.
216
217 **Expression of *P. aeruginosa* genes significantly changed over 7 d in the EVPL biofilm.**
218
219 PCA of PA14 gene expression identified distinct transcriptomes at 24h, 48h and 7d PI (Figure
220 S1). There was no clear difference between samples from different lungs, indicating
221 variation between time points was much larger than between-lung variation. *P. aeruginosa*
222 grown for 24 h was the most distinct from other time points, supported by hierarchical
223 clustering and Pearson's correlation coefficient analyses (Figure S1; Figure S2). Differential
224 expression analysis similarly showed the greatest difference at 24 h vs 48h or 7d PI, with the
225 smallest number of significantly differentially expressed genes (DEGs) arising between 48 h
226 and 7 d (Figure 1).
227
228 Overall, more genes were found to be significantly overexpressed than underexpressed
229 between sequential time points (Figure 1A), suggesting gene expression increased over time
230 in the EVPL biofilm. While some genes showed changes in expression over all three time
231 points, there were also unique DEGs identified between each time point comparison (Figure
232 1B). This indicated there were different dynamics in gene expression changes across the
233 three time points.
234

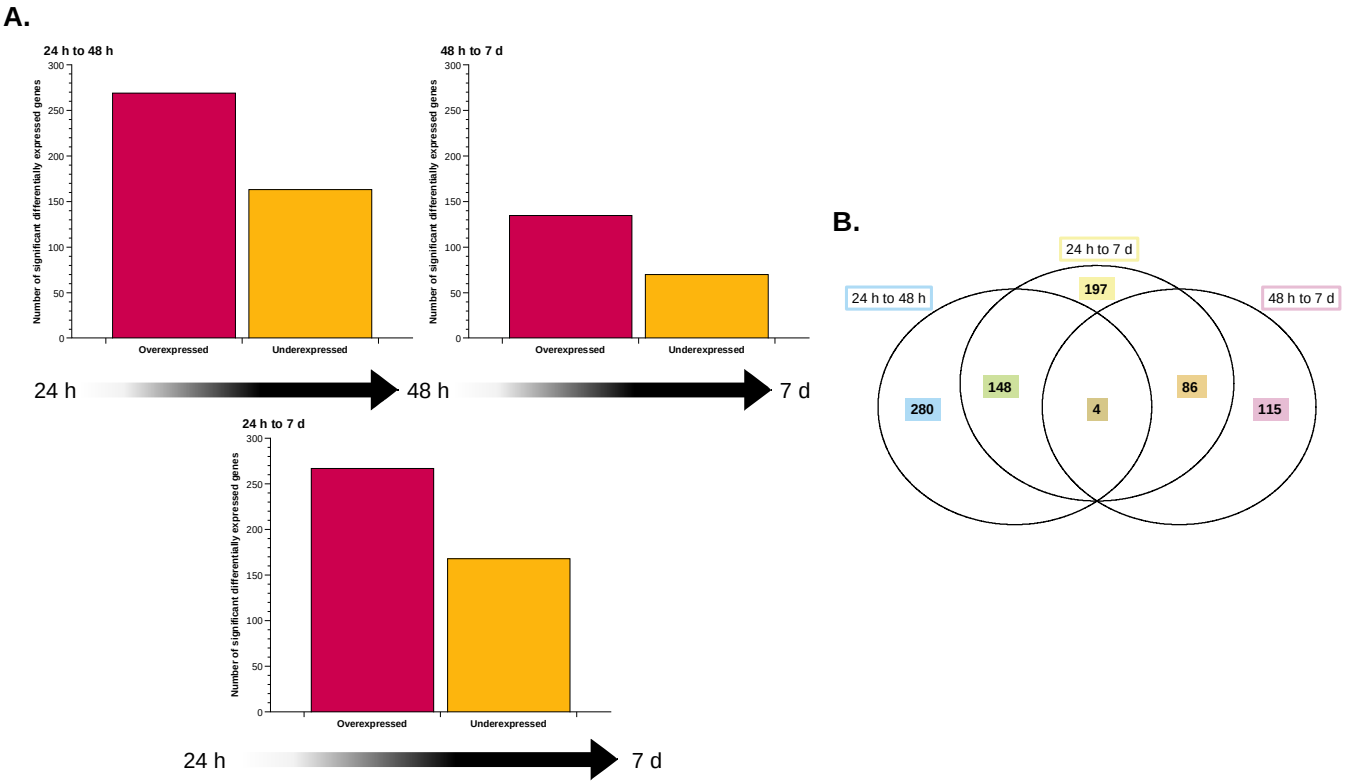

Figure 1. The number of *Pseudomonas aeruginosa* PA14 significant differentially expressed genes (DEGs) ($P < 0.05$, $|\log_2 \text{fold change}| \geq 1.5$) in each time contrast in the *ex vivo* pig lung (EVPL) model biofilm. RNA was sequenced from three tissue-associated biofilms from each of two independent pig lungs, per time point. **(A)** The number of significantly overexpressed genes (pink, left bar) and significantly underexpressed genes (yellow, right bar) in each time contrast. Significant DEGs were determined at 48 h compared with 24 h (showing change from 24 h to 48 h), at 7 d compared with 48 h (48 h to 7 d), and at 7 d compared with 24 h (24 h to 7 d). **(B)** A Venn diagram of the number of significant DEGs. Shared genes were either significantly overexpressed or underexpressed in all contrasts compared. Genes that were significant in multiple contrasts but in opposing directions were not considered shared.

Changes in *P. aeruginosa* gene expression followed seven different profiles with functional implications.

To further investigate the gene expression changes over time in the EVPL-associated biofilm, expression profiles were determined based on shared, unique and non-significant changes between time point comparisons. We classified the DEGs into seven profiles based on the direction and magnitude of their change in expression 24 - 48h and 48h - 7d, outlined in Table 1.

Table 1. *Pseudomonas aeruginosa* PA14 gene expression profiles identified in the *ex vivo* pig lung-associated biofilm at 24 h, 48 h and 7 d. The graphical representations demonstrate the changes in expression of genes over the three time points. Below each graph is the number of significant differentially expressed genes found to follow that expression profile.

Profile number	Gene expression profile	Graphical representation
1	Significant change in expression 24 h to 48 h, then a significant change in the **same** direction 48 h to 7 d. Results in significant change 24 h to 7 d.	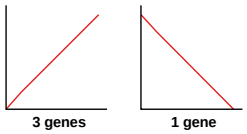
2	Significant change in expression 24 h to 48 h, which is **maintained** 48 h to 7 d (no significant change). Results in significant change 24 h to 7 d.	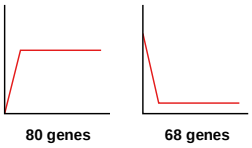
3	No significant change in expression 24 h to 48 h, then a significant change 48 h to 7 d. Results in significant change 24 h to 7 d.	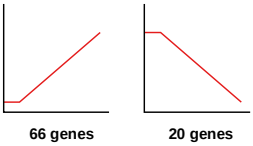
4	Significant change in expression 24 h to 48 h, then a small but not significant change in the **opposite** direction 48 h to 7 d. Results in no significant change 24 h to 7 d.	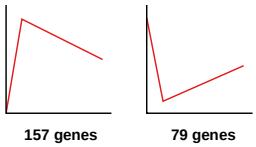
5	Small but not significant change in expression 24 h to 48 h, then a small but not significant change in the **same** direction 48 h to 7 d. Results in overall significant change 24 h to 7 d.	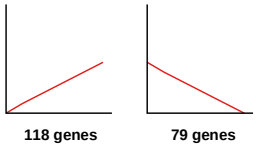
6	Small but not significant change in expression 24 h to 48 h, then a significant change in the **opposite** direction 48 h to 7 d. Results in no significant change 24 h to 7 d.	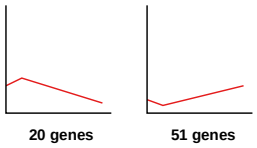
7	Significant change in expression 24 h to 48 h, then a significant change in the **opposite** direction 48 h to 7 d. Results in no significant change 24 h to 7 d.	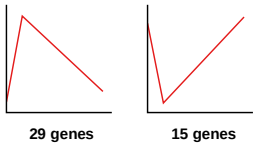

Four genes were found to be significantly differentially expressed in the same direction 24 h - 48 h, and then 48 h - 7 d (Figure 1B), classified as expression profile 1 (Table 1), however

there was no functional association between these genes (Table S2). A second profile where gene expression changed in the same direction over 7 d but at a slower rate was identified, resulting in a significant change 24 h - 7 d (profile 5; Table 1). KEGG enrichment analysis found four pathways significantly enriched ($P < 0.05$) for this profile, including degradation of aromatic compounds and benzoate degradation (Figure 2B). All significant DEGs in the degradation of aromatic compounds pathway were linked to benzoate degradation. Arginine biosynthesis was also significantly enriched (Figure 2B), and two of the associated significant DEGs that reduced in expression over time were arginine fermentation enzymes [32]: *arcB* (-2.25 $\log_2$ fold change (FC)) and *arcC* (-2.16 $\log_2$FC), which have been shown to be induced under stress [33, 34]. Additionally, sulfur metabolism was significantly enriched for this profile as well as expression profile 2 (Figure 2), where there was a significant increase in expression 24 h - 48 h that was maintained for 7 d (Table 1).

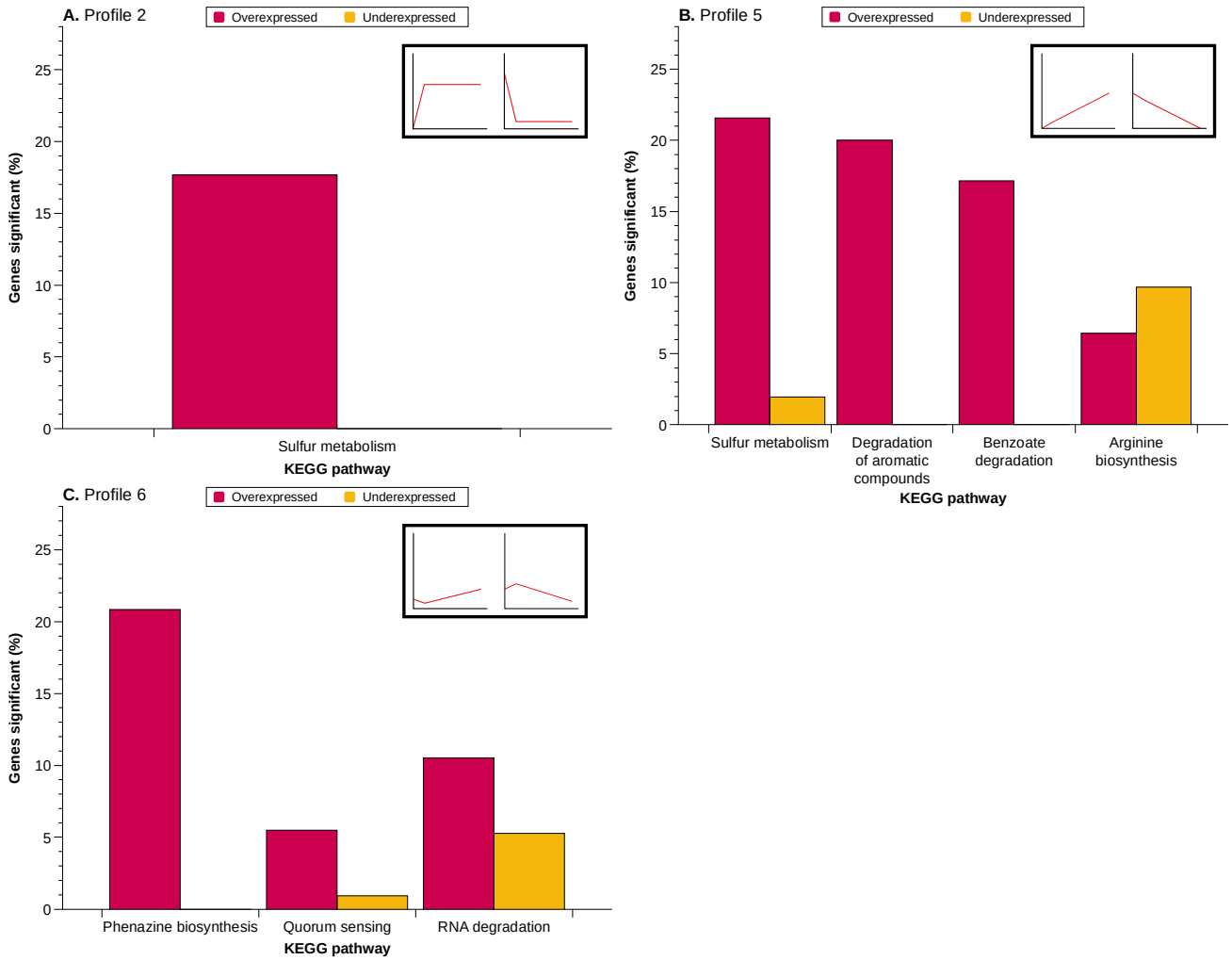

Figure 2. Significantly enriched ($P < 0.05$) *Pseudomonas aeruginosa* PA14 Kyoto Encyclopedia of Genes and Genomes (KEGG) pathways found for gene expression profiles in the *ex vivo* pig lung-associated biofilm over 24h, 48 h and 7 d. The expression of significantly differentially expressed genes over the three time points was investigated and separated into seven different profiles, three of which were found to involve sufficient genes associated with KEGG pathways for pathways to be significantly enriched. The bars show the percentage of significant differentially expressed genes associated with each enriched pathway ($P < 0.05$, $|\log_2 \text{fold change}| \geq 1.5$); those overexpressed (left bar) and underexpressed (right bar) are shown by different colours (see key). The graphical representation of the gene expression profile is shown in the top right of each graph; the left graph shows the profile of overexpressed genes, and the right graph shows the profile of underexpressed genes. **(A)** Significantly enriched KEGG pathway following expression profile 2. **(B)** Significantly enriched KEGG pathways following profile 5. **(C)** Significantly enriched KEGG pathways following profile 6.

Gene expression profile 6 was the only other group where there were significantly enriched KEGG pathways ($P < 0.05$), involving a significant change in expression 48 h - 7 d (Table 1; Figure 2C). This included phenazine biosynthesis and QS (Figure 2C); all phenazine biosynthesis significant DEGs were also associated with the QS pathway.

Sulfur metabolism was upregulated over 7 d in the EVPL-associated biofilm.

As expression changes 24 h - 7 d appeared to have the greatest functional implications, KEGG enrichment analysis was performed on all significant DEGs that arose in this comparison. There were no *P. aeruginosa* PA14 pathways significantly enriched 24 h - 48 h, and those found between 48 h and 7 d were comparable to expression profile 6 (Figure 2C; Figure S3). Four pathways were significantly enriched 24 h - 7 d in the EVPL-associated biofilm ($P < 0.05$): sulfur metabolism, ATP-binding cassette (ABC) transporters, degradation of aromatic compounds and nitrogen metabolism (Figure 3).

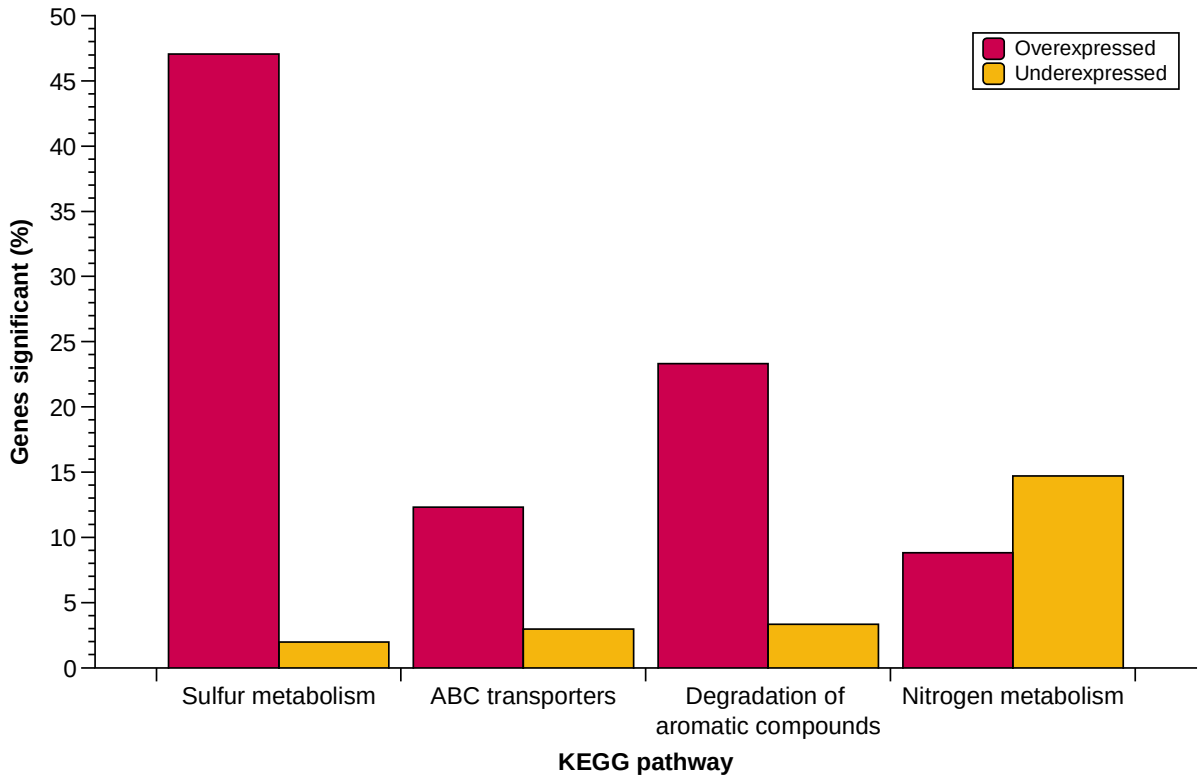

Figure 3. Significantly enriched (*P* < 0.05) *Pseudomonas aeruginosa* PA14 Kyoto encyclopedia of genes and genomes (KEGG) pathways in the *ex vivo* pig lung-associated biofilm from 24 h to 7 d. Each bar shows the percentage of genes associated with each pathway that were significantly differentially expressed (*P* < 0.05, $|\log_2 \text{fold change}| \geq 1.5$). The overexpressed genes (left bar) and underexpressed genes (right bar) are show by different colour bars (see key).

The greatest percentage of associated significant DEGs was for sulfur metabolism (Figure 3): 47.06% of sulfur metabolism genes were significantly overexpressed in the EVPL biofilm 24 h - 7 d, suggesting this pathway was upregulated. This included sulfate transport genes *cysA*, *cysW* and *cysT* (3.04, 2.87, and 3.14 $\log_2$FC respectively). There was only one associated gene significantly reduced in expression at 7 d: the sulfite/nitrate reductase PA14_10550 (-1.56 $\log_2$FC). The majority of the significantly differentially expressed ABC transporter genes were involved in sulfur metabolism. However, three phosphate-specific transporter genes

314 were also significantly overexpressed: *pstB* (1.52 log_2FC), *pstA* (1.83 log_2FC), and *pstC* (1.88
315 log_2FC).
316
317 Nitrogen metabolism was the only significantly enriched pathway where more significant
318 DEGs decreased in expression 24 h - 7 d than increased (Figure 3). Expression of genes in the
319 *P. aeruginosa* nitrogen metabolism operons responsible for a shift towards anaerobic
320 respiration in CF sputum (*nor*, *nir*, *nap*, and *nos*, [35]) was investigated, but no clear, shared
321 pattern of upregulation or downregulation was observed (Table S1).
322
323 **Antimicrobial tolerance increased in the *P. aeruginosa* PA14 EVPL-associated biofilm over**
324 **7 d despite limited antimicrobial resistance gene expression changes.**
325
326 Our previous work highlighted significant differential expression of antimicrobial resistance
327 (AMR) genes in the *P. aeruginosa* PA14 EVPL-associated biofilm compared with *in vitro*
328 growth at both 24 h and 48 h [8]. Therefore, we next aimed to investigate whether any of
329 the changes in gene expression found over 7 d were linked to AMR.
330
331 Three AMR genes were found to be significantly reduced in expression over time in the EVPL
332 biofilm (Table 2) and none were found to be significantly increased. The full AMR gene list
333 investigated is shown in Table S3. The *brc-1* gene, encoding a major facilitator superfamily
334 (MFS) transporter associated with bicyclomycin resistance [36], was significantly reduced in
335 expression 24 h - 7 d. The other two significant DEGs: *mexG* and *arnA*, which encode a
336 transmembrane protein associated with multiple efflux pumps and a bifunctional UDP-
337 glucuronic acid decarboxylase/UDP-4-amino-4-deoxy-L-arabinose formyltransferase [1],

were significantly reduced in expression 24 h - 48 h. The enzyme encoded by *arnA* is involved in lipid A modifications, linked to cationic antimicrobial peptide (CAMP) resistance [37, 38], and was previously shown to be significantly overexpressed in the EVPL-associated biofilm compared with *in vitro* SCFM growth at 24 h [8].

Table 2. *Pseudomonas aeruginosa* PA14 antibiotic resistance associated genes found to be significantly differentially expressed in at least one contrast in the *ex vivo* pig lung-associated biofilm between 24 h, 48 h and 7 d. The gene expression group denotes the expression profile the gene belonged to, with the corresponding expression plot (Table 1). The $\log_2$ fold change ($\log_2$FC) in the contrast where the gene was significantly differentially expressed is shown. A gene was considered significantly differentially expressed if $|\log_2 \text{ fold change}| \geq 1.5$ and $P < 0.05$.

Locus tag	Gene name	Gene product	Gene expression group	Time: Log_2FC
PA14_09540	*mexG*	Transmembrane protein	4	24 h to 48 h: -1.52
PA14_18350	*arnA*	Bifunctional UDP-glucuronic acid decarboxylase/UDP-4-amino-4-deoxy-L-arabinose formyltransferase	4	24 h to 48 h: -1.59
PA14_10470	*bcr-1*	MFS transporter	5	24 h to 7 d: -2.49

To determine whether reduction in expression of the CAMP resistance-associated gene *arnA* had a phenotypic effect, *P. aeruginosa* PA14 was grown as a biofilm on the EVPL tissue for 24 h, 48 h or 7 d, and exposed to each of two clinically relevant CAMPs, colistin and polymyxin B, for a further 24 h. *P. aeruginosa* grown as a biofilm for 24 h could not be recovered following treatment with 256 µg ml^{-1} colistin (Figure 4A). However, after 48 h

initial growth, PA14 was inconsistently recovered (Figure 4B). By 7 d, all biofilm populations were able to tolerate 256 µg ml^{-1} colistin (Figure 4C). This pattern was comparable to the response to 256 µg ml^{-1} polymyxin B (Figure 4). The increased polymyxin tolerance was a contrast to the limited changes in AMR gene expression observed, and the significantly reduced expression of *arnA*. This may be linked to persistence of non-dividing cells in the biofilm population. As we do not know the rate of *P. aeruginosa* division in the EVPL model, it may be possible that there is an early increase in efflux pump and *arnA* expression that modifies the cell surface to a CAMP-tolerant phenotype, which is maintained. Alternatively, there may be other phenotypic factors driving increased tolerance, such as the established biofilm providing protection against CAMPs.

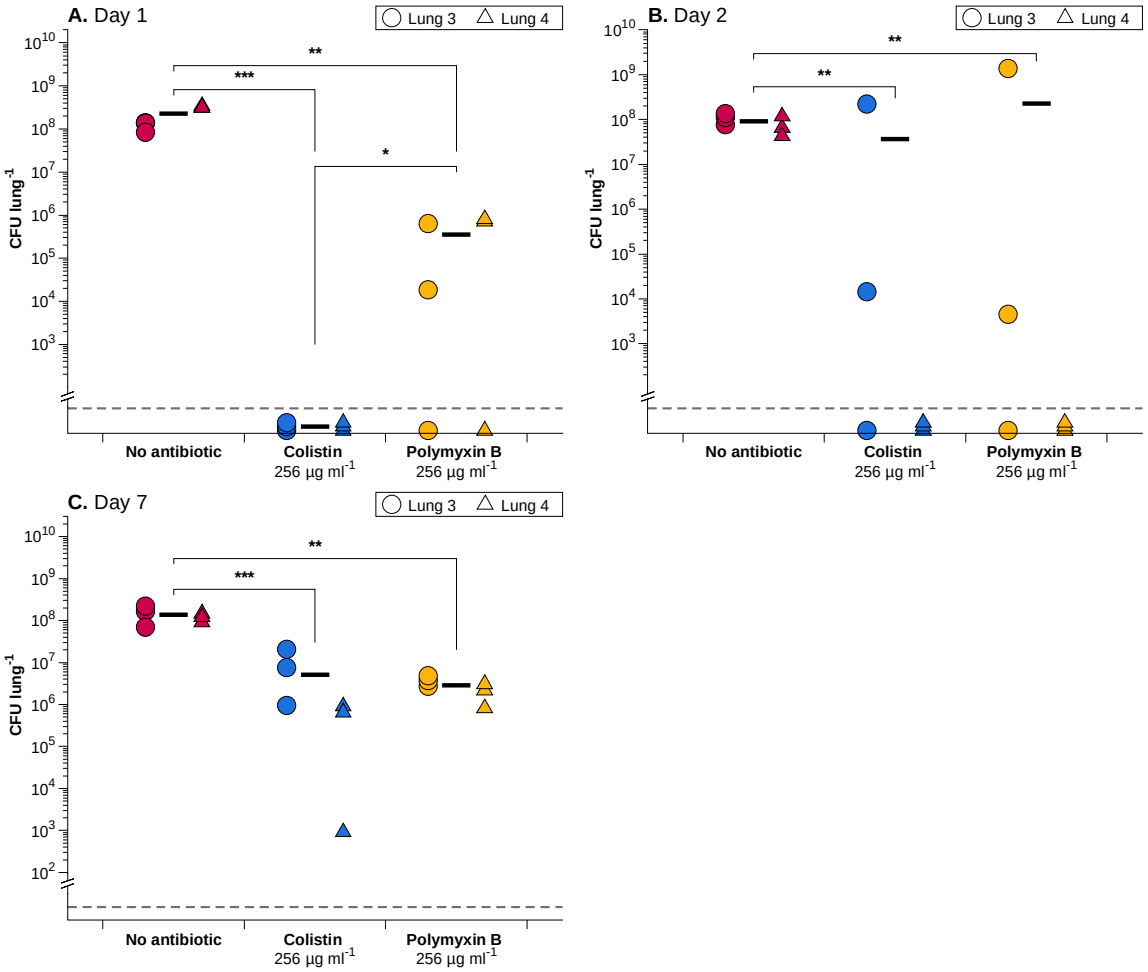

Figure 4. The colony forming units per lung tissue piece (CFU lung^{-1}) for the *Pseudomonas aeruginosa* PA14 *ex vivo* pig lung tissue-associated biofilm of different ages following no antibiotic treatment, treatment with 256 µg ml^{-1} colistin, or 256 µg ml^{-1} polymyxin B. Three replicates from each of two independent pig lungs, shown by different shaped data points (see key), were used. The *P. aeruginosa* PA14 biofilms were grown in the *ex vivo* pig lung (EVPL) model for **(A)** 24 h **(B)** 48 h **(C)** 7 d, then exposed to either phosphate-buffered saline (PBS) as a negative control (no antibiotic; pink), 256 µg ml^{-1} colistin (blue), or 256 µg ml^{-1} polymyxin B (yellow) for a further 24 h. The CFU lung^{-1} was then determined and is shown on the graphs, data points below the dashed horizontal line represent samples where no CFU were detected. The asterisks represent a significant difference between treatments determined using post-hoc Tukey HSD tests following ANOVA (* = $P < 0.05$). **(A)** Day 1 ANOVA: treatment $F_{2,12} = 30.32$, $P < 0.01$; lung $F_{1,12} = 0.15$, $P = 0.71$; interaction $F_{2,12} = 0.04$, $P = 0.96$. **(B)** Day 2 ANOVA: treatment $F_{2,12} = 10.53$, $P < 0.01$; lung $F_{1,12} = 5.76$, $P = 0.03$; interaction $F_{2,12} = 1.26$, $P = 0.32$. **(C)** Day 7 ANOVA: treatment $F_{2,12} = 14.51$, $P < 0.01$; lung $F_{1,12} = 4.12$, $P = 0.07$; interaction $F_{2,12} = 2.30$, $P = 0.14$.

A mature, structured *P. aeruginosa* biofilm was maintained for 7 d on the surface of the EVPL tissue, associated with reduced expression of Pel biosynthesis.

Therefore, to further explore the increase in antimicrobial tolerance observed over 7 d, gene expression changes in QS and biofilm formation pathways were investigated. Both are involved in the establishment of antibiotic tolerant, chronic *P. aeruginosa* infections in the CF lung, and the EVPL biofilm has been shown to capture these aspects of *in vivo* infection at 48 h PI [8]. There were no overall differences in QS gene expression in any of the time point comparisons (Figure 5; Figure S4; Figure S5). As our previous study demonstrated that the expression of QS-regulated genes in the EVPL-associated biofilm at 48 h PI is comparable to human infection [19], this indicates a representative biofilm infection was maintained for 7 d (Figure S4). Other genes associated with *P. aeruginosa* PA14 virulence factor production were also investigated, including those involved in motility, type III secretion, type VI secretion, and alginate biosynthesis, however no significant differential expression was found.

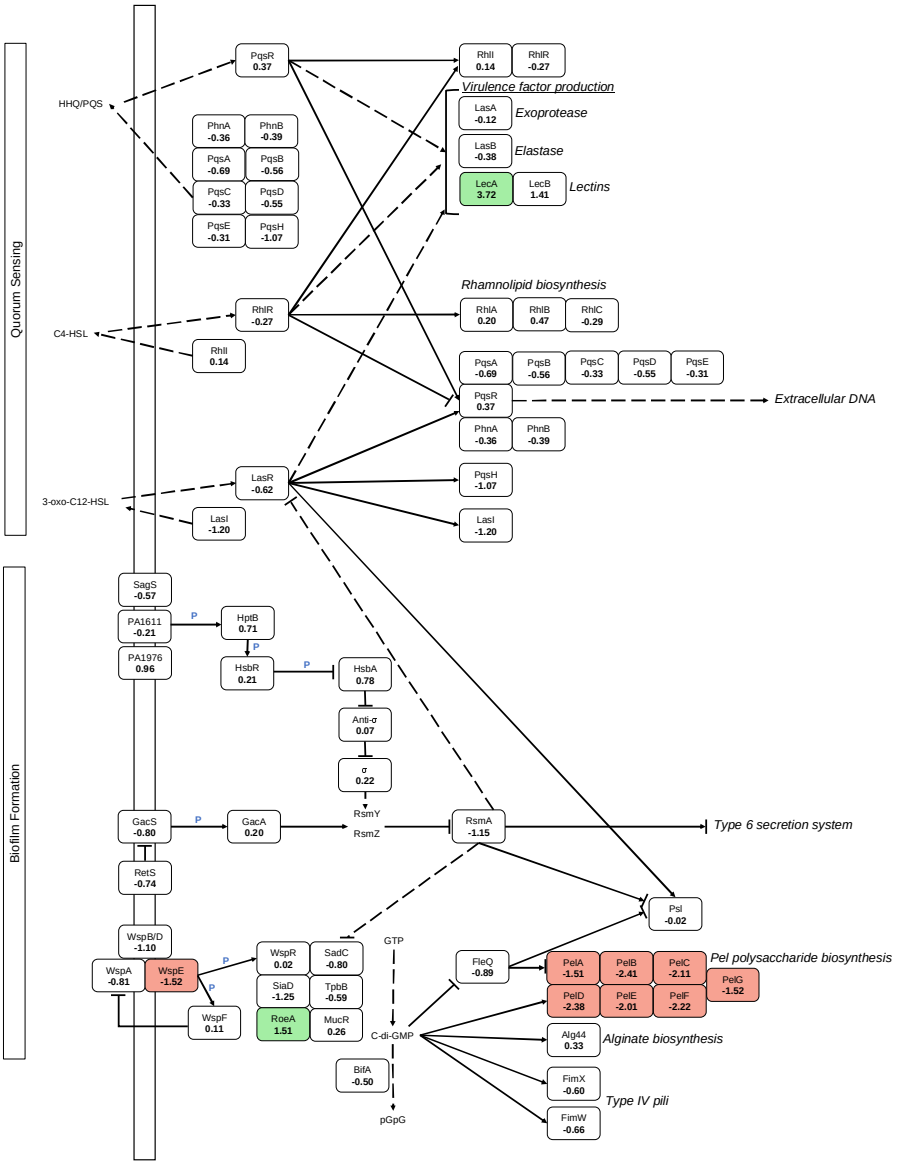

Figure 5. Pathway map of the gene expression changes in the *Pseudomonas aeruginosa* PA14 Kyoto Encyclopedia of Genes and Genomes (KEGG) biofilm formation and quorum sensing (QS) pathways in the *ex vivo* pig lung-associated biofilm from 24 h to 7 d. The diagram shows all genes involved in each pathway, including associated signalling pathways and the Pel exopolysaccharide biosynthesis pathway. The $\log_2$ fold change value from 24 h to 7 d is shown below each gene name. The genes shown in red were significantly underexpressed, and genes shown in green were significantly overexpressed (significance: $P < 0.05$, $|\log_2 \text{fold change}| \geq 1.5$). The blocked arrows represent gene activation, and the dashed arrows show indirect gene activation. The solid, blocked lines (ending with |, not an arrow) show inhibition, and the dashed, blocked lines show indirect inhibition. The blue 'P' represents phosphorylation.

In contrast, all genes in the operon for biosynthesis of the biofilm exopolysaccharide Pel were found to be significantly reduced in expression 24 h - 7 d (Figure 5), five of which were also significantly reduced 24 h - 48 h (Figure S5). This suggests that the biofilm matrix was formed in the first 24 h, and maintained for 7 d. To investigate this hypothesis, the biofilm formed at each of these time points was visualised using scanning electron microscopy (SEM). Uninfected tissue was imaged as a negative control (Figure S6). A biofilm could not be imaged at 24 h, however a dense, structured *P. aeruginosa* PA14 biofilm was clear at 48 h (Figure 6), consistent with previous work [9]. The biofilm population was maintained at 7 d, where a very dense biofilm of *P. aeruginosa* PA14 cells was observed (Figure 7).

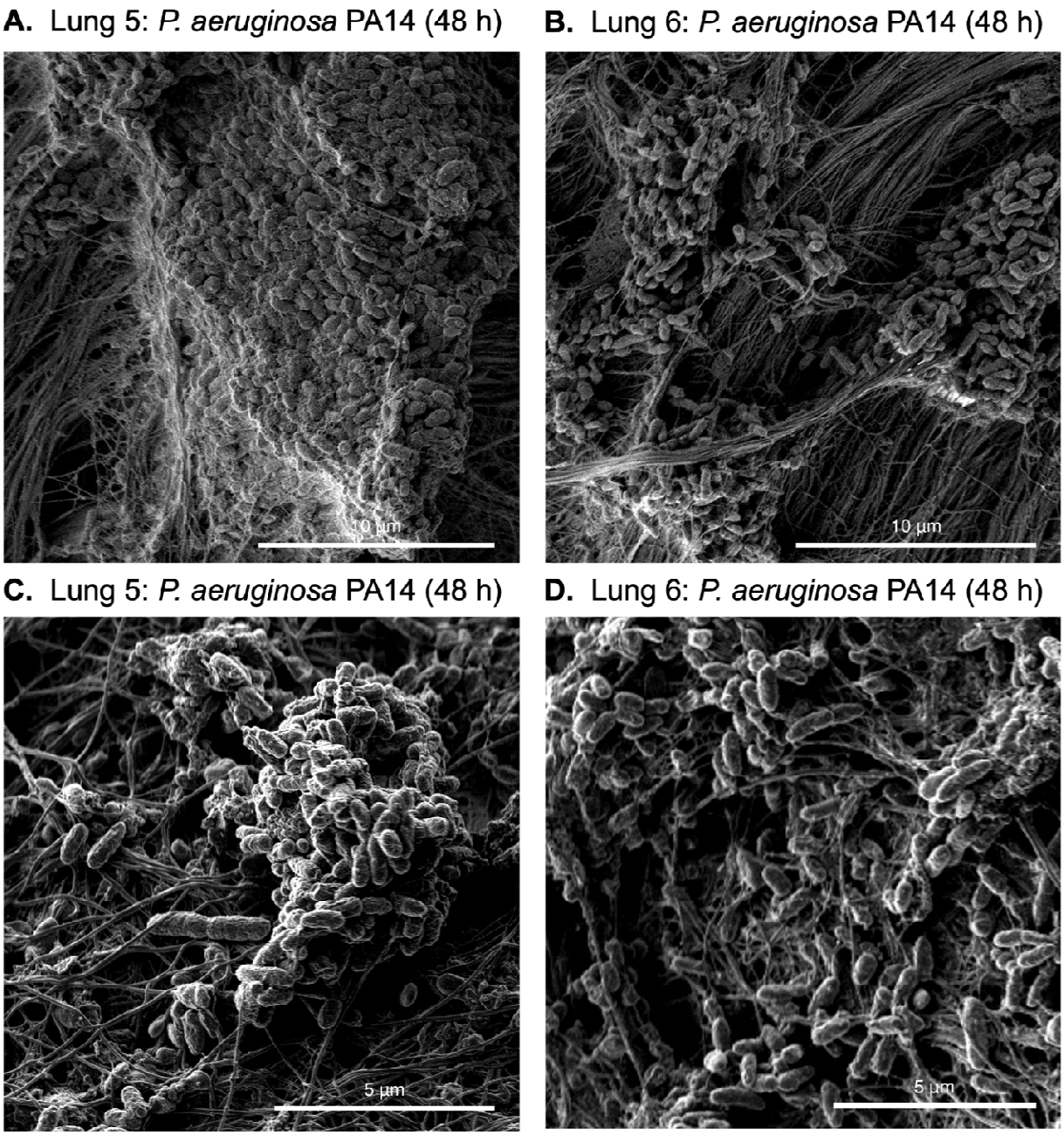

Figure 6. Scanning electron micrographs of *Pseudomonas aeruginosa* PA14 biofilms associated with *ex vivo* pig lung (EVPL) bronchiolar tissue 48 h after infection. Images were taken from biofilms formed on tissue from two independent pig lungs: **(A, C)** lung 5 **(B, D)** lung 6, showing biofilm aggregates of cells. The thicker fibrous structures are consistent with the appearance of collagen fibrils under SEM, while the finer fibrous structures may be individual collagen fibres and/or elastin fibres – both major components of the connective tissue in bronchioles. Scale bars are shown. Images were taken using a Zeiss Gemini electron microscope with an InLens detector, at 1kV, and analysed using Omero5.6 [30].

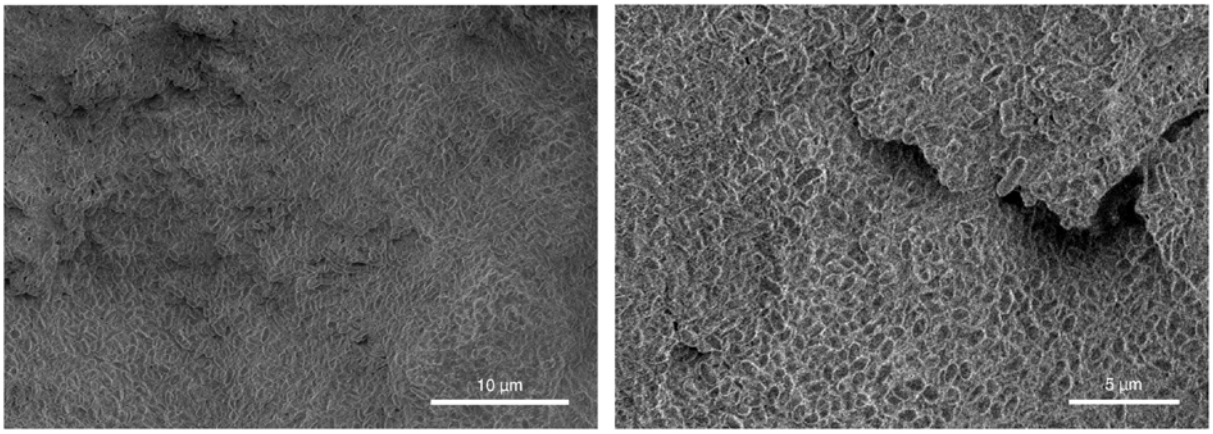

Figure 7. Scanning electron micrographs of *Pseudomonas aeruginosa* PA14 biofilms associated with *ex vivo* pig lung (EVPL) bronchiolar tissue 7 d post infection Scale bars are shown. Images were taken using a Zeiss Gemini electron microscope with an InLens detector, at 1kV, and analysed using Omero5.6 [30]

Discussion

We have used RNA sequencing data [8] to investigate *P. aeruginosa* biofilm infection in the EVPL model over 7 d. We identified upregulation of several non-stress related pathways, including sulfur metabolism, and demonstrated increased antibiotic tolerance. SEM confirmed that a dense, mature biofilm was formed by 48 h that was maintained at 7 d PI, with no visible indications of stress. Our findings show that the EVPL model provides an environment for *P. aeruginosa* biofilm formation that once a clinically relevant biofilm has formed at 48 h [8], it can be maintained as a chronic-like infection for 7 d.

Sulfur metabolism had the highest percentage of significant DEGs associated of all the significantly enriched KEGG pathways over time. More specifically, all genes in the sulfur

transporter operon associated with cysteine biosynthesis: *cysTWA*, were found to be significantly overexpressed 24 h - 7 d. In *E. coli,* upregulation of this operon has been linked to sulfate starvation [39]. However, investigation of the sulfate starvation response in *P. aeruginosa* PAO1 and a cystic fibrosis isolate found cysteine biosynthesis genes were only weakly upregulated when sulfate was limited [40]. *P. aeruginosa* PA14 upregulation of sulfur metabolism in SCFM has actually been linked to a shift towards anaerobic respiration [41], which is associated with increased antibiotic tolerance [42]. There have also been links made with iron starvation and sulfur metabolism. However, during iron starvation, proteins involved in cysteine biosynthesis and sulfur assimilation are reduced [43].

Additionally, during infection of the CF lung, there is an increase in sulfation of the airway mucins compared with a non-CF lung [44, 45], in part caused by inflammation [46], that chronically adapted *P. aeruginosa* can use. It has also been shown that there is enough inorganic sulfate in CF sputum to facilitate *P. aeruginosa* growth without mucin as a source [47], therefore sulfur starvation is unlikely in this environment. Therefore, upregulation of sulfur metabolism in the EVPL biofilm was more likely a result of a change in lifestyle, such as anaerobic respiration, than nutrient starvation. Hence, our findings may further support the progression of *P. aeruginosa* biofilm infection in the EVPL model as capturing the lifestyle changes observed in CF. However, sulfur and oxygen availability in the EVPL biofilm should be determined in the future to confirm this hypothesis.

Our previous work demonstrated that the EVPL biofilm may more accurately recapitulate *P. aeruginosa* QS gene expression in CF sputum than other *in vitro* models [8], so *P. aeruginosa* PA14 changes in expression of genes in the three QS pathways over 7 d were investigated:

465 LasI/R, RhlI/R, and PQS, and no significant changes were found. Other regulatory pathways
466 involved in lifestyle changes, including the switch from acute to chronic infection, were also
467 investigated however no clear differences in expression were found either. There were also
468 no significant changes in virulence factor gene expression. It is known that as part of
469 adaptation to the CF lung and formation of a chronic infection, virulence factor production is
470 significantly reduced [48]. Therefore, *P. aeruginosa* may have already switched off virulence
471 factor production by 24 h as it formed the established biofilm visualised at 48 h, hence no
472 change in gene expression was observed. This is supported by the findings in our previous
473 study, in which we found two of the major protease-encoding genes *lasA* and *lasB* were
474 significantly underexpressed in the EVPL-associated biofilm compared with SCFM *in vitro*
475 growth at both 24 h and 48 h [8]. This may also explain why no significant differential
476 expression was observed in regulatory pathways including QS. Additionally, adaptation to
477 the CF lung is also linked with mutations in *P. aeruginosa* virulence pathways [48], therefore
478 future work looking at the accumulation of mutations over 7 d in the EVPL-associated *P.*
479 *aeruginosa* biofilm would provide further insight.
480
481 In contrast, significant changes in the expression of biofilm-associated genes were found in
482 the EVPL PA14 biofilm population over 7 d. Pel biosynthesis was significantly downregulated
483 24 h - 48 h, then maintained at the same expression level 48 h - 7 d, which resulted in
484 significant downregulation 24 h - 7 d. This indicated that Pel production was reduced after
485 24 h of infection, then maintained from 48 h onwards. Pel is a biofilm exopolysaccharide
486 essential for PA14 biofilm development and is only expressed during biofilm growth [49, 50].
487 Whilst our results do not confirm there was not any Pel being produced at the later time
488 points, they indicate less than the initial stage of infection in the EVPL model. This may have

been caused by upregulation of Pel biosynthesis as the biofilm was established at 24 h, which was reduced once the biofilm was formed at 48 h and maintained at this lower level over the remaining 5 d. This hypothesis was supported by SEM images of the biofilm, which showed a dense, structured *P. aeruginosa* biofilm already present at 48 h.

Taking this into account, following formation of a biofilm, gene expression analysis indicated that the focus may have shifted from production of the biofilm matrix to biofilm maintenance and maturation 48 h - 7 d. Significant upregulation of two lectin genes was also observed in the lung-associated biofilm 24 h - 7 d, and 24 h - 48 h. Both have been associated with a mature biofilm; *lecA* is indicated to play a role in the formation of a mature biofilm architecture [51], and *lecB* has been shown to be involved in increased cell and exopolysaccharide retention in biofilms [52]. This retention may also have been associated with the reduction in Pel production, as less new Pel would be required if the exopolysaccharide already produced was being retained. The proposed maintenance of a mature biofilm structure was also accompanied by increased antimicrobial tolerance.

In our first study of *P. aeruginosa* PA14 gene expression in the EVPL model compared with *in vitro* SCFM growth, we found that the EVPL growth environments cued differential expression of a number of AMR genes despite no antibiotic exposure, at both 24 h and 48 h [8]. However, only three genes involved in AMR were differentially expressed over 7 d in the EVPL biofilm, suggesting differential expression of resistance-associated genes cued by the environment is unlikely to be dynamic and remains consistent throughout 7 d infection. The significantly differentially expressed AMR genes that were found included significant

reduction in expression of two individual antibiotic resistance genes: *arnA* and *bcr-1*, associated with resistance to CAMPs [38] and bicyclomycin [36] respectively.

Despite these findings, increased tolerance to colistin and polymyxin B was observed at 7 d, compared with 24 h and 48 h. It is hypothesised that the formation of a biofilm, of which the matrix facilitates antibiotic resistance [2], may have resulted in other mechanisms of antibiotic resistance being downregulated as they were not required. This would provide explanation as to why expression of AMR genes was reduced once a biofilm had formed, and the matrix was no longer being rapidly produced. This finding would further support the use of biofilm disrupters to improve treatment regimens, as the *P. aeruginosa* cells within the biofilm may not be expressing genes associated with antibiotic resistance and are thus more susceptible to treatments.

However, it must also be considered that there were other indirect mechanisms of antibiotic resistance that were found to be significantly overexpressed in the EVPL biofilm, which are associated with potential environmental pressures. Phosphate transporters were significantly overexpressed from 24 h to 7 d, indicative of phosphate stress. Under phosphate stress *P. aeruginosa* has been shown to undergo lipid modifications that confer resistance to polymyxin B. There is a transition from phospholipids to glycolipids, which confer protection against polymyxin B [53]. Therefore, this differential expression may also be responsible for or involved in, the increased antibiotic tolerance observed. Future investigation of *P. aeruginosa* lipid modifications in the EVPL model environment would further understanding. This analysis has however indicated that these pathways may be

induced, thus investigation of lipid modifications cued by the EVPL model may highlight novel treatment targets.

In summary, we have demonstrated that there are changes in the *P. aeruginosa* lung-associated biofilm transcriptome in the EVPL model over 24h - 7 d of infection. We have identified an increase in polymyxin tolerance 48h - 7d that is accompanied by an upregulation of sulfur metabolism and phosphate transport, rather than AMR-associated genes. Whilst further work is required to fully determine the chronic-like phenotype formed by 7 d PI, our results highlight a key further time point to address future research questions related to chronic lung infection using the EVPL model. Introduction of other factors that influence *P. aeruginosa* gene expression in the CF lung, such as other microbes, may reveal other changes in the biofilm population over time that facilitate survival in these conditions *in vivo*. Further understanding of these mechanisms will provide better understanding to eradicate or prevent chronic *P. aeruginosa* infections in the CF lung.

Acknowledgements

We would like to thank all at Steve Quigley & Sons butchers for donating the pig lungs used for this work, and Leo Eberl for the bacterial strain used. We would also like to thank Jenna Lam for her help with the RNA extraction process and Blessing Anonye for her guidance. We also acknowledge the help of the Media Preparation Facility in the School of Life Sciences at the University of Warwick, with special thanks to Cerith Harries and Caroline Stewart, and the Electron Microscopy Research Technology Platform at the University of Warwick for use of the Zeiss Gemini scanning electron microscope. This work was supported by an MRC New

Investigator Research Grant (grant number MR/R001898/1) awarded to F.H., a PhD studentship from the BBSRC Midlands Integrative Biosciences Training Partnership (MIBTP) awarded to N.E.H., a PhD studentship from the MRC Doctoral Training Programme in Interdisciplinary Biomedical Research awarded to R.G.M., and the University of Warwick as part of F.A.'s MBio degree in Biomedical Science.

Author Contributions

N.E.H. and F.H. designed research; N.E.H., F.A., and R.G.M. performed research; N.E.H. and F.A. analyzed data; N.E.H. and F.A. wrote the paper; N.E.H., F.A., R.G.M., and F.H. edited the paper.

Conflicts of Interest

The authors declare no conflict of interest.

References

1. Winsor, G.L., et al., *Enhanced annotations and features for comparing thousands of Pseudomonas genomes in the Pseudomonas genome database.* Nucleic Acids Research, 2016. **44**(D1): p. D646-D653.
2. Høiby, N., et al., *Antibiotic resistance of bacterial biofilms.* International Journal of Antimicrobial Agents, 2010. **35**(4): p. 322-332.
3. Wardell, S.J.T., et al., *Genome evolution drives transcriptomic and phenotypic adaptation in Pseudomonas aeruginosa during 20 years of infection.* Microbial Genomics, 2021. **7**(11).
4. Hogardt, M. and J. Heesemann, *Microevolution of Pseudomonas aeruginosa to a Chronic Pathogen of the Cystic Fibrosis Lung*, in *Between Pathogenicity and Commensalism*. 2011, Springer Berlin Heidelberg. p. 91-118.

5. Rossi, E., et al., *Pseudomonas aeruginosa adaptation and evolution in patients with cystic fibrosis.* Nature Reviews Microbiology, 2021. **19**(5): p. 331-342.
6. Jiricny, N., et al., *Loss of Social Behaviours in Populations of Pseudomonas aeruginosa Infecting Lungs of Patients with Cystic Fibrosis.* PLoS ONE, 2014. **9**(1): p. e83124.
7. Cornforth, D.M., et al., *Pseudomonas aeruginosa transcriptome during human infection.* PNAS, 2018. **115**(22): p. E5125-E5134.
8. Harrington, N.E., J.L. Littler, and F. Harrison, *Transcriptome Analysis of Pseudomonas aeruginosa Biofilm Infection in an Ex Vivo Pig Model of the Cystic Fibrosis Lung.* Applied and Environmental Microbiology, 2022. **88**(3).
9. Harrington, N.E., E. Sweeney, and F. Harrison, *Building a better biofilm - Formation of in vivo-like biofilm structures by Pseudomonas aeruginosa in a porcine model of cystic fibrosis lung infection.* Biofilm, 2020. **2**.
10. Liberati, N.T., et al., *An ordered, nonredundant library of Pseudomonas aeruginosa strain PA14 transposon insertion mutants.* Proceedings of the National Academy of Sciences, 2006. **103**(8): p. 2833-2838.
11. Liberati, N.T., et al. *PA14 transposon insertion mutant library*. 2006 [cited 2022 10/05/2022]; Available from: http://pa14.mgh.harvard.edu/cgi-bin/pa14/home.cgi.
12. Palmer, K.L., L.M. Aye, and M. Whiteley, *Nutritional Cues Control Pseudomonas aeruginosa Multicellular Behavior in Cystic Fibrosis Sputum.* Journal of Bacteriology, 2007. **189**(22): p. 8079-8087.
13. Harrison, F. and S.P. Diggle, *An ex vivo lung model to study bronchioles infected with Pseudomonas aeruginosa biofilms.* Microbiology, 2016. **162**(10): p. 1755-1760.
14. Harrington, N.E., et al., *Antibiotic Efficacy Testing in an Ex vivo Model of Pseudomonas aeruginosa and Staphylococcus aureus Biofilms in the Cystic Fibrosis Lung.* Journal of Visualized Experiments, 2021(167).
15. Andrews, S. *FastQC: a quality control tool for high throughput sequence data.* 2018; Available from: https://www.bioinformatics.babraham.ac.uk/projects/fastqc/.
16. Bolger, A.M., M. Lohse, and B. Usadel, *Trimmomatic: a flexible trimmer for Illumina sequence data.* Bioinformatics, 2014. **30**(15): p. 2114-2120.
17. Kopylova, E., L. Noé, and H. Touzet, *SortMeRNA: fast and accurate filtering of ribosomal RNAs in metatranscriptomic data.* Bioinformatics, 2012. **28**(24): p. 3211-3217.
18. Kim, D., et al., *Graph-based genome alignment and genotyping with HISAT2 and HISAT-genotype.* Nature Biotechnology, 2019. **37**(8): p. 907-915.
19. Li, H. *A toolkit for processing sequences in FASTA/Q formats.* 2015; Available from: https://github.com/lh3/seqtk.
20. Li, H., *Aligning sequence reads, clone sequences and assembly contigs with BWA-MEM.* ArXiv, 2013. **00**.
21. Liao, Y., G.K. Smyth, and W. Shi, *The R package Rsubread is easier, faster, cheaper and better for alignment and quantification of RNA sequencing reads.* Nucleic Acids Research, 2019. **47**(8): p. e47-e47.
22. Love, M.I., W. Huber, and S. Anders, *Moderated estimation of fold change and dispersion for RNA-seq data with DESeq2.* Genome Biology, 2014. **15**(12).
23. Kassambara, A. *ggpubr: "ggplot2" based publication ready plots. R package version 0.4.0.* 2020; Available from: https://cran.r-project.org/package=ggpubr.
24. Chen, H., *VennDiagram: Generate High-Resolution Venn and Euler Plots. R package version 1.7.0.* 2021.

25. Yu, G., et al., *ClusterProfiler: an R package for comparing biological themes among gene clusters.* OMICS, 2012. **16**: p. 284-287.
26. Alcock, B.P., et al., *CARD 2020: antibiotic resistome surveillance with the comprehensive antibiotic resistance database.* Nucleic Acids Research, 2019.
27. Kanehisa, M. and S. Goto, *KEGG: Kyoto Encyclopedia of Genes and Genomes.* Nucleic Acids Research, 2000. **28**(1): p. 27-30.
28. Kanehisa, M., *Toward understanding the origin and evolution of cellular organisms.* Protein Science, 2019. **28**(11): p. 1947-1951.
29. Kanehisa, M., et al., *KEGG: integrating viruses and cellular organisms.* Nucleic Acids Research, 2021. **49**(D1): p. D545-D551.
30. Goldberg, I.G., et al., *The Open Microscopy Environment (OME) Data Model and XML file: open tools for informatics and quantitative analysis in biological imaging.* Genome Biology, 2005. **6**(5): p. R47.
31. Adalsteinsson, D. and P. Schultz, *The DataGraph Manual.* 2020.
32. Schreiber, K., et al., *Anaerobic Survival of Pseudomonas aeruginosa by Pyruvate Fermentation Requires an Usp-Type Stress Protein*. Journal of Bacteriology, 2006. **188**(2): p. 659-668.
33. Eschbach, M., et al., *Long-Term Anaerobic Survival of the Opportunistic Pathogen Pseudomons aeruginosa via Pyruvate Fermentation.* Journal of Bacteriology, 2004. **186**(14).
34. Mercenier, A., et al., *Regulation of enzyme synthesis in the arginine deiminase pathway of Pseudomonas aeruginosa.* Journal of Bacteriology, 1980. **144**(1).
35. Rossi, E., et al., *High-resolution in situ transcriptomics of Pseudomonas aeruginosa unveils genotype independent patho-phenotypes in cystic fibrosis lungs.* Nature Communications, 2018. **9**(1).
36. Fonseca, E.L., et al., *Full characterization of the integrative and conjugative element carrying the metallo-β-lactamase blaSPM-1 and bicyclomycin bcr1 resistance genes found in the pandemic Pseudomonas aeruginosa clone SP/ST277.* Journal of Antimicrobial Chemotherapy, 2015. **70**(9): p. 2547-2550.
37. Roy, S., et al., *Transcriptional expression of PmrB and arnA within polymyxin-resistant nosocomial isolates of Pseudomonas aeruginosa from India.* Journal of Microbiology and Infectious Diseases, 2018. **8**(3): p. 61-68.
38. Gutu, A.D., et al., *Pseudomonas aeruginosa High-Level Resistance to Polymyxins and Other Antimicrobial Peptides Requires cprA, a Gene That Is Disrupted in the PAO1 Strain.* Antimicrobial Agents and Chemotherapy, 2015. **59**(9): p. 5377-5387.
39. Gyaneshwar, P., et al., *Sulfur and Nitrogen Limitation in Escherichia coli K-12: Specific Homeostatic Responses.* Journal of Bacteriology, 2005. **187**(3): p. 1074-1090.
40. Tralau, T., et al., *Transcriptomic Analysis of the Sulfate Starvation Response of Pseudomonas aeruginosa.* Journal of Bacteriology, 2007. **189**(19): p. 6743-6750.
41. Tata, M., et al., *RNASeq Based Transcriptional Profiling of Pseudomonas aeruginosa PA14 after Short- and Long-Term Anoxic Cultivation in Synthetic Cystic Fibrosis Sputum Medium.* PLOS ONE, 2016. **11**(1): p. e0147811.
42. Schobert, M. and D. Jahn, *Anaerobic physiology of Pseudomonas aeruginosa in the cystic fibrosis lung.* International Journal of Medical Microbiology, 2010. **300**(8): p. 549-556.
43. Nelson, C.E., et al., *Proteomic Analysis of the Pseudomonas aeruginosa Iron Starvation Response Reveals PrrF Small Regulatory RNA-Dependent Iron Regulation*

of Twitching Motility, Amino Acid Metabolism, and Zinc Homeostasis Proteins. Journal of Bacteriology, 2019. **201**(12).

44. Cheng, P.W., et al., *Increased sulfation of glycoconjugates by cultured nasal epithelial cells from patients with cystic fibrosis.* Journal of Clinical Investigation, 1989. **84**(1): p. 68-72.
45. Xia, B., et al., *Altered O-glycosylation and sulfation of airway mucins associated with cystic fibrosis.* Glycobiology, 2005. **15**(8): p. 747-775.
46. Lamblin, G., et al., *Human airway mucin glycosylation: A combinatory of carbohydrate determinants which vary in cystic fibrosis.* Glycoconjugate Journal, 2001. **18**(9): p. 661-684.
47. Robinson, C.V., et al., *Desulfurization of mucin by Pseudomonas aeruginosa: influence of sulfate in the lungs of cystic fibrosis patients.* Journal of Medical Microbiology, 2012. **61**(12): p. 1644-1653.
48. Smith, E.E., et al., *Genetic adaptation by Pseudomonas aeruginosa to the airways of cystic fibrosis patients.* Proceedings of the National Academy of Sciences, 2006. **103**(22): p. 8487-8492.
49. Colvin, K.M., et al., *The Pel Polysaccharide Can Serve a Structural and Protective Role in the Biofilm Matrix of Pseudomonas aeruginosa.* PLoS Pathogens, 2011. **7**(1): p. e1001264.
50. Marmont, L.S., et al., *PelA and PelB proteins form a modification and secretion complex essential for Pel polysaccharide-dependent biofilm formation in Pseudomonas aeruginosa.* Journal of Biological Chemistry, 2017. **292**(47): p. 19411-19422.
51. Diggle, S.P., et al., *The galactophilic lectin, LecA, contributes to biofilm development in Pseudomonas aeruginosa.* Environmental Microbiology, 2006. **8**(6): p. 1095-1104.
52. Passos Da Silva, D., et al., *The Pseudomonas aeruginosa lectin LecB binds to the exopolysaccharide Psl and stabilizes the biofilm matrix.* Nature Communications, 2019. **10**(1).
53. Jones, R.A., et al., *Phosphorus stress induces the synthesis of novel glycolipids in Pseudomonas aeruginosa that confer protection against a last-resort antibiotic.* The ISME Journal, 2021. **15**(11): p. 3303-3314.